EUROPEAN ORGANIZATION FOR NUCLEAR RESEARCH

CERN-EP/86-154
9 October 1986

EXPERIMENTAL DETERMINATION OF THE BRANCHING RATIOS $p\bar{p} \to 2\pi^0$, $\pi^0\gamma$, AND 2γ AT REST

L. Adiels[2], G. Backenstoss[1], I. Bergström[2], S. Carius[2,5], S. Charalambous[3], M.D. Cooper[1,5], Ch. Findeisen[1], D. Hatzifotiadou[3], M. Hugi[1], A. Kerek[2], H.O. Meyer[1,8], P. Pavlopoulos[4], J. Repond[1,6], L. Tauscher[1], D. Tröster[1,4], M.C.S. Williams[1,7] and K. Zioutas[3]

ABSTRACT

The branching ratios of $p\bar{p}$ annihilations into the neutral final states $2\pi^0$, $\pi^0\gamma$, and 2γ are measured by stopping antiprotons in liquid hydrogen. They are $B_{2\pi^0} = (2.06 \pm 0.14) \times 10^{-4}$, $B_{\pi^0\gamma} = (1.74 \pm 0.22) \times 10^{-5}$, and $B_{\gamma\gamma} < 1.7 \times 10^{-6}$ (95% c.l.).

(Submitted to Physics Letters B)

1) Institute for Physics, University of Basle, Switzerland
2) Research Institute of Physics, Stockholm, Sweden
3) University of Thessaloniki, Greece
4) CERN, Geneva, Switzerland
5) Los Alamos National Laboratory, Los Alamos, N. Mex., USA
6) Now at Argonne National Laboratory, Argonne, Ill., USA
7) Now at Dept. of Physics, University of California, Davis, Calif., USA
8) Indiana University, Bloomington, Ind., USA

We report a partial result from an experiment whose aim is to study the decay at rest of the proton–antiproton system into photons and uncharged mesons. In particular, we discuss the branching ratios into the neutral final states $2\pi^0$, $\pi^0\gamma$, 2γ, and $3\pi^0$. Although these decays are relatively rare, they are detected with enhanced sensitivity because of their kinematic peculiarities. The experiment benefits from the intense, low-energy antiproton beam from the LEAR facility at CERN and from the use of a high resolution π^0 spectrometer.

Of the above branching ratios, all but $p\bar{p} \to 2\gamma$ have been measured previously: the branching ratio for $2\pi^0$ with partly contradictory results [1–3], and the $\pi^0\gamma$ branching ratio quite indirectly [3]. The aim of this work is to clarify the problem of P-wave annihilation in liquid hydrogen for the channel $p\bar{p} \to \pi\pi$ by the measurement of $p\bar{p} \to 2\pi^0$, and to check the predictions of the vector–meson dominance model for the branching ratios into $\pi^0\gamma$ and 2γ.

The experiment has been carried out with a 300 MeV/c $\bar{p}$-beam from LEAR. The beam of about 10^5 $\bar{p}$ per second is stopped in a 0.5 cm^3 volume inside a liquid–hydrogen target. The detector set-up is designed to measure photons from the decay of annihilation products. It consists of one array of bismuth germanate (BGO) crystals and another array of lead-glass (LG) blocks. The BGO array contains seven hexagonal prisms; its effective solid angle of 21.0 ± 0.6 msr is defined by imposing conditions on the sharing of deposited energy among the detector elements. The LG array is composed of four adjacent rows of 40 lead-glass wedges arranged around the target volume as shown in ref. [4], subtending an angle of 120° transverse to the beam direction. The effective width of the detector in the beam direction is defined by conditions on energy sharing between elements; the corresponding solid angle is 420 ± 13 msr. Further details of the detector set-up are given elsewhere [4–6]. In this measurement the BGO system was positioned opposite the centre of the LG detector. The data reported here have been collected in December 1983 and correspond to a total of 2.95×10^9 stopped antiprotons, corrected for the dead time of the data acquisition system ($\leq 10\%$).

Off-line sorting of the full data sample is designed to suppress final states other than those treated in this report. Events which are selected off-line for the present study are required to be triple coincidences, i.e. they must consist of one photon (γ_1) in the BGO system and two distinct photons (γ_2,γ_3) in the LG detector, separated by at least 12° in order to prevent the two γ-showers from overlapping. The photons in the LG detector have to represent a decaying π^0. Hence only (γ_2,γ_3)-pairs are selected whose invariant mass is $95 < m_{\gamma_2\gamma_3} < 175$ MeV/c^2, corresponding to a 4σ cut in the invariant-mass distribution around the π^0 mass. Subsequently, energies and directions of the two γ's are subject to a kinematical fit with the constraint $m_{\gamma_2\gamma_3} = m_{\pi^0}$, and events with $\chi^2 > 3.8$ are rejected. From this fit the π^0 momentum $\mathbf{p}_{\pi^0}$ is deduced. In order to discriminate against annihilation channels containing heavy mesons, a condition is imposed on the missing mass M of each event

$$M = 2[(2m_p - E_{\pi^0} - E_{\gamma_1})^2 - (\mathbf{p}_{\pi^0} + \mathbf{p}_{\gamma_1})^2]^{1/2} < 250\,\mathrm{MeV}/c^2\,, \tag{1}$$

where m_p is the proton mass. The cut-off value for M in eq. (1) is dictated by the experimental resolution. The special kinematics of the processes $p\bar{p} \to 2\pi^0$ and $p\bar{p} \to \pi^0\gamma$ allows further rejection by requiring the angle between $\mathbf{p}_{\pi^0}$ and $\mathbf{p}_{\gamma_1}$ to be greater than 166° and by imposing the condition $E_{\gamma_1} > 600$ MeV.

Selecting events in the manner described leads to a π^0 momentum spectrum as shown in fig. 1. As expected, the only remaining feature is a peak at $p_{\pi^0} = 930$ MeV/c, corresponding to both $p\bar{p} \to 2\pi^0$ and $p\bar{p} \to \pi^0\gamma$. Rejecting π^0 momenta below 850 MeV/c (arrow in fig. 1) in order to suppress contributions from background such as $p\bar{p} \to 3\pi^0$, the same data sample is plotted versus E_{γ_1} in fig. 2. This spectrum is expected to contain a peak at 933.4 MeV from $p\bar{p} \to \pi^0\gamma$ and a continuous distribution from $p\bar{p} \to 2\pi^0$ downward from 933.4 MeV; it constitutes the basis for the following analysis.

In order to deduce branching ratios for individual channels, their expected contributions to the E_{γ_1} spectrum for a given branching ratio is calculated using Monte Carlo techniques. In this simulation, our knowledge of the performance of the experimental apparatus is taken into account. A superposition of the calculated energy distributions, with branching ratios adjusted to fit the data, directly yields the desired results.

When simulating the contributions of the annihilation channels of interest and of background channels to the γ_1 energy spectrum, events with the appropriate kinematics are generated at random, smeared with the experimental resolution of the BGO system [4], and histogrammed with a weight that is, apart from phase space, determined by the following factors: i) the probability that three photons are contained within the geometrical acceptance of the LG detector and the BGO system; for the channel $p\bar{p} \to \pi^0\gamma$ this factor is $(4.10 \pm 0.18) \times 10^{-4}$; for continuous distributions it depends on the photon energies; ii) the probability (0.95 ± 0.01) that none of the three photons converts before reaching the detectors; and iii) a correction (0.88 ± 0.01) for events lost owing to cuts in the off-line sorting of the LG detector, i.e. the minimum separation of two γ's, the missing mass and kinematical fit conditions, and the minimum π^0 momentum accepted. The compounded error of the corrections (i)–(iii) amounts to 4.9%.

In the course of the simulation it has been found that uncorrelated photon pairs γ_2, γ_3 contribute less than 1% to the E_{γ_1} spectrum and that the background channel $p\bar{p} \to \pi^0\eta(\eta \to 2\gamma)$ can be neglected. Since other conceivable background channels, such as $p\bar{p} \to 4\pi^0$, $\pi^+\pi^-2\pi^0$, $2\pi^0\eta$, and $\pi^0 f^0(f^0 \to 2\pi^0)$, fall outside the accepted kinematical conditions, the only background contribution may come from $p\bar{p} \to 3\pi^0$ and, possibly, $p\bar{p} \to \pi^0\omega(\omega \to \pi^0\gamma)$. Since the latter two processes yield contributions to the γ_1 spectrum that are similar in shape, the only background channel introduced in the final analysis is $p\bar{p} \to 3\pi^0$.

The three simulated contributions described above are added, with variable branching ratios, to best fit the spectrum in fig. 2. Thereby, the integral for $E_{\gamma_1} > 600$ MeV (the total number of counts in the spectrum) is kept constant, reducing the number of free parameters to two. This procedure yields the branching ratios B_ν, i.e. the fraction of all $p\bar{p}$ annihilations leading to the channel ν:

$$B_{\pi^0\gamma} = (1.9 \pm 0.9) \times 10^{-5}$$

$$B_{2\pi^0} = (2.19 \pm 0.26) \times 10^{-4}$$

$$B_{3\pi^0} < 5.2 \times 10^{-3} \text{ (95\% c.l.)}$$

The errors contain contributions from statistics, from systematics (the compounded error of the weight used in the simulation), and from a 1% uncertainty in the absolute energy calibration of the BGO, since the best-fit values depend on the relative position of the simulated E_{γ_1} spectrum with respect to the measured one. In order to test the independence of the quoted results on the range of γ_1 energies considered in the analysis, the whole procedure was repeated with lower limits for E_{γ_1} of 500, 700, and 800 MeV, yielding consistent results. For $B_{3\pi^0}$ only an upper limit is given, since it is compatible with zero because of the very large error, and since a possible, unknown admixture from the channel $p\bar{p} \to \pi^0\omega(\omega \to \pi^0\gamma)$ could not be separated.

It should be noted that the evidence for the presence of $p\bar{p} \to \pi^0\gamma$ in the triple coincidence data sample is strongly dependent on the energy calibration, as can be seen from fig. 1. This correlation may be removed by using a completely different data sample where one photon in the BGO system and only one photon in the LG detector is required. Only those events are selected with both photon energies, E_{γ_1} and E_{γ_2}, greater than 450 MeV and with the angle between their directions greater than 170°, corresponding to very asymmetric decays of the π^0's. The upper end of the sum energy spectrum, $E_{tot} = E_{\gamma_1} + E_{\gamma_2}$, is shown in fig. 3. The E_{tot} distributions for the channels $p\bar{p} \to \pi^0\gamma$, $p\bar{p} \to 2\pi^0$, and $p\bar{p} \to 3\pi^0$ were simulated and fitted to the data analogously to the procedure followed for the triple coincidences. As can be seen from figs. 2 and 3, the three channels contribute in very different ways to the E_{γ_1} and E_{tot} distributions. Fitting the three branching ratios simultaneously to the E_{γ_1} and E_{tot} spectra removes the correlations of parameters, which are present when fitting the distributions individually. Such a simultaneous fit was carried out, fitting also the energy calibrations for the two distributions. The result is:

$$B_{\pi^0\gamma} = (1.74 \pm 0.20 \pm 0.09) \times 10^{-5} \qquad (2)$$

$$B_{2\pi^0} = (2.06 \pm 0.09 \pm 0.10)\, 2 \times 10^{-4} \qquad (3)$$

$$B_{3\pi^0} < 5.0 \times 10^{-3}\, (95\%\ \text{c.l.})\,. \qquad (4)$$

The first error is the parabolic statistical error of a MINOS [7] analysis, while the second one is the systematic error of 4.9% discussed above. This result is fully consistent with the result obtained from the E_{γ_1} spectrum alone. This agreement proves the consistency of our procedure in analysing the data, considering the fact that the offline treatment and the correction factors applied to the two-fold coincidence sample differ substantially from those used for the triple coincidences.

The limit on $B_{3\pi^0}$ set by this experiment, eq. (4), is not necessarily in contradiction with the earlier result $B_{3\pi^0} = (7.6 \pm 2.3) \times 10^{-3}$ [8], considering that the present experiment samples only a small region of phase space. Our result for $B_{2\pi^0}$, eq. (3), is in qualitative agreement with two previous measurements, $(6 \pm 4) \times 10^{-4}$ [3] and $(1.4 \pm 0.3) \times 10^{-4}$ [2], but more than two standard deviations smaller than the value $[(4.8 \pm 1.0) \times 10^{-4}]$ from ref. [1]. The only previously determined value for $B_{\pi^0\gamma}$, $B_{\pi^0\gamma} = (1.5 \pm 0.7) \times 10^{-4}$ [3] is about two standard deviations higher than our result, eq. (2).

In the sum energy spectrum, fig. 3, the channel $p\bar{p} \to 2\gamma$ should lead to a peak which, owing to the experimental resolution, has a width of 80 MeV (FWHM), and which is located at E_{tot} = 1877 MeV, i.e. in a region of the spectrum where there is very little contribution from any other process (arrow in fig. 3). Such a peak is not observed. The upper limit for the corresponding branching ratio is

$$B_{2\gamma} < 1{,}7 \times 10^{-6}\, (95\%\ \text{c.l.})\,. \qquad (5)$$

To our knowledge, this is the first experimental information available on the production of this final state in liquid hydrogen.

In the framework of the vector-meson dominance model [9], which assumes that the photon coupling to hadronic states is dominated by single vector-meson intermediate states, the branching ratio $B_{\pi^0\gamma}$ is linked to $B_{\pi^0\varrho}$ and $B_{\pi^0\omega}$ (explicit expressions are given in ref. [10]). Aside from kinematical factors, the relation contains the coupling constants $f_{\varrho\gamma}$ and $f_{\omega\gamma}$, and the relative phase, $\cos\beta$, between isoscalar and isovector contributions. The latter is unknown but $\cos\beta = 1$ is favoured by SU(3). Using $\cos\beta = 1$, $B_{\pi^0\varrho^0} = (1.4 \pm 0.2) \times 10^{-2}$ [11], and assuming $B_{\pi^0\omega} = 0.3B_{\pi^0\varrho^0}$ [6], yields $B_{\pi^0\gamma^0} \approx 1.1 \times 10^{-4}$, which is a factor of 4 larger than the value given in eq. (2). The same model also leads to a connection between $B_{2\gamma}$, $B_{2\varrho}$, and $B_{\varrho\omega}$. In this case the calculated value of $B_{2\gamma} < 10^{-6}$ [10] is compatible with the upper limit, eq. (5), found in this experiment.

The annihilation $p\bar{p} \to 2\pi^0$ cannot proceed from an initial S state of the $p\bar{p}$ system. This restriction does not hold for $p\bar{p} \to \pi^+\pi^-$, which therefore may proceed from S- and P-states. Assuming charge independence, the fraction R of annihilations originating from P-wave initial states with respect to all annihilations into $\pi\pi$ is $R = 3B_{2\pi^0}/(B_{\pi^+\pi^-} + B_{2\pi^0})$. Using $B_{\pi^+\pi^-} = (32 \pm 3) \times 10^{-4}$ [11] and $B_{2\pi^0}$ from eq. (3), we find $R = (18 \pm 2)\%$. If $B_{2\pi^0}$ is taken from other sources [1-3] the resulting values for R vary between 13% and 50%. An upper limit for P-wave annihilations in liquid hydrogen was obtained for $p\bar{p} \to K_SK_S$ (P-wave only) and $p\bar{p} \to K_SK_L$ (S- and P-wave) [12], allowing for at most a few per cent P-wave annihilation if only selection rules are considered. However, a recent measurement with a gas target and the selection of initial P waves by X-ray observation [13] revealed that the process $p\bar{p} \to K_SK_S$ is already suppressed by about a factor of 10 with respect to $p\bar{p} \to K_SK_L$. This leads to an upper limit for P-wave annihilation which is ten times higher and, hence, to agreement with our result for $p\bar{p} \to \pi\pi$. Unless there is a special annihilation mechanism to enhance P-wave with respect to S-wave annihilations in the case of $p\bar{p} \to \pi\pi$ we conclude that P-wave annihilations in liquid hydrogen might in general be of the order of 20%. This would then also be in qualitative agreement with detailed calculations of the atomic cascade for liquid hydrogen [14].

This experiment was supported by the Swiss National Science Foundation, the Swedish Research Council, and the Greek Administration for Research and Technology. We wish to thank CERN for the support and the hospitality we have received. We are also indebted to K. Agehed and A. Engström (Stockholm), K. Iconomou (Thessaloniki) and H. Krause (Basle) for mechanical-engineering support.

REFERENCES

[1] S. Devons et al., Phys. Rev. Lett. **27** (1971) 1614.

[2] G. Bassompierre et al., Proc. 4th European Antiproton Symposium, Strasburg, 1978 (ed. A. Fridman) (CNRS, Paris, 1979), vol. I, p. 139.

[3] G. Backenstoss et al., Nucl. Phys. **228B** (1983) 424.

[4] L. Adiels et al., Nucl. Instrum. Methods **A244** (1986) 380.

[5] C. Findeisen, PhD Thesis, University of Basle (1986).

[6] S. Carius, PhD Thesis, Royal Institute of Technology, Stockholm (1986).

[7] F. James and M. Roos, Comput. Phys. Commun. **10** (1975) 343.

[8] S. Devons et al., Phys. Lett. **47B** (1973) 271.

[9] J.J. Sakurai, Ann. Phys. (NY) **11** (1960) 1.

[10] B. Delcourt, J. Layssac and E. Pelaquier, Proc. Workshop on Physics at LEAR, Erice, 1981 (eds. U. Gastaldi and R. Klapisch) (Plenum Press, New York, 1982), p. 305.

[11] C. Baltay et al., Phys. Rev. Lett. **15** (1965) 532.

[12] R. Bizzarri, Proc. Symposium on Nucleon–Antinucleon Annihilation, Chexbres, 1972 (ed. L. Montanet) (CERN 72-10 Geneva, 1972), p. 161.

[13] S. Ahmad et al., Proc. Physics with Antiprotons at LEAR (ed. U. Gastaldi) (Éditions Frontières, Gif-sur-Yvette, 1985), p. 353.

[14] E. Borie, same Proc. as ref. [10], p. 185.

Figure captions

Fig. 1 : π^0 momentum spectrum for the triple coincidence data sample after applying selective cuts. Events to the left of the arrow are neglected in the subsequent analysis. The solid curve is a Gaussian fit to the data.

Fig. 2 : Spectrum of E_{γ_1}, the energy of the photon detected by the BGO system, for the triple coincidence sample. Calculated individual contributions are shown for $p\bar{p} \rightarrow \pi^0\gamma$ (---), $p\bar{p} \rightarrow 2p^0$ (—·—·), and $p\bar{p} \rightarrow 3\pi^0$ (····). The solid curve is the sum of all three final states.

Fig. 3 : Spectrum of the sum $E_{tot} = E_{\gamma_1} + E_{\gamma_2}$ for the double coincidence sample. Calculated individual contributions are shown for $p\bar{p} \rightarrow \pi^0\gamma$ (---), $p\bar{p} \rightarrow 2\pi^0$ (—·—·), and $p\bar{p} \rightarrow 3\pi^0$ (····). The solid curve is the sum of all three final states. The arrow points to the energy where a peak with a FWHM of 80 MeV from $p\bar{p} \rightarrow 2\gamma$ is expected.

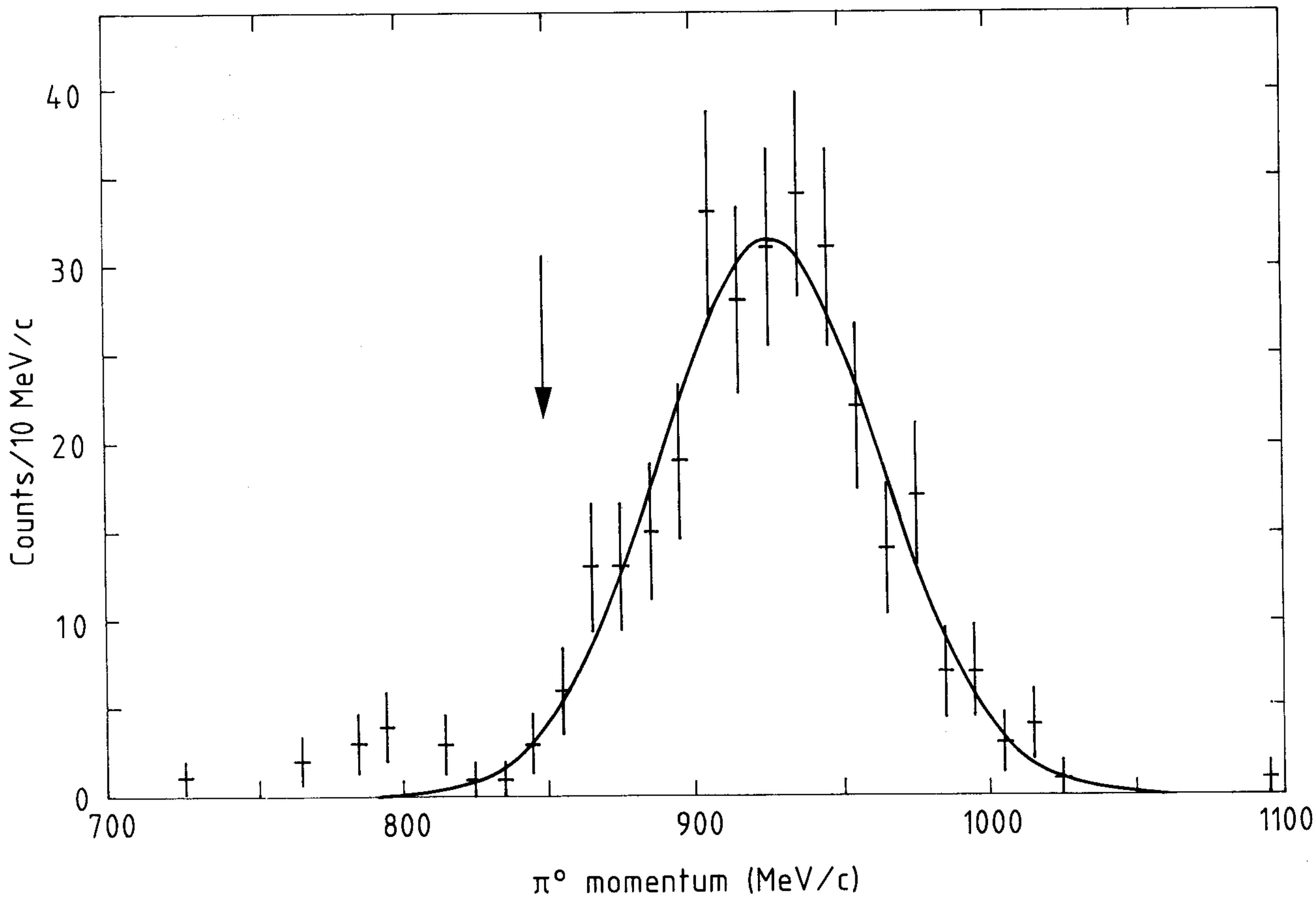

40
30
20
10
0
Counts/10 MeV/c
700
800
900
1000
1100
π° momentum (MeV/c)

Fig. 1

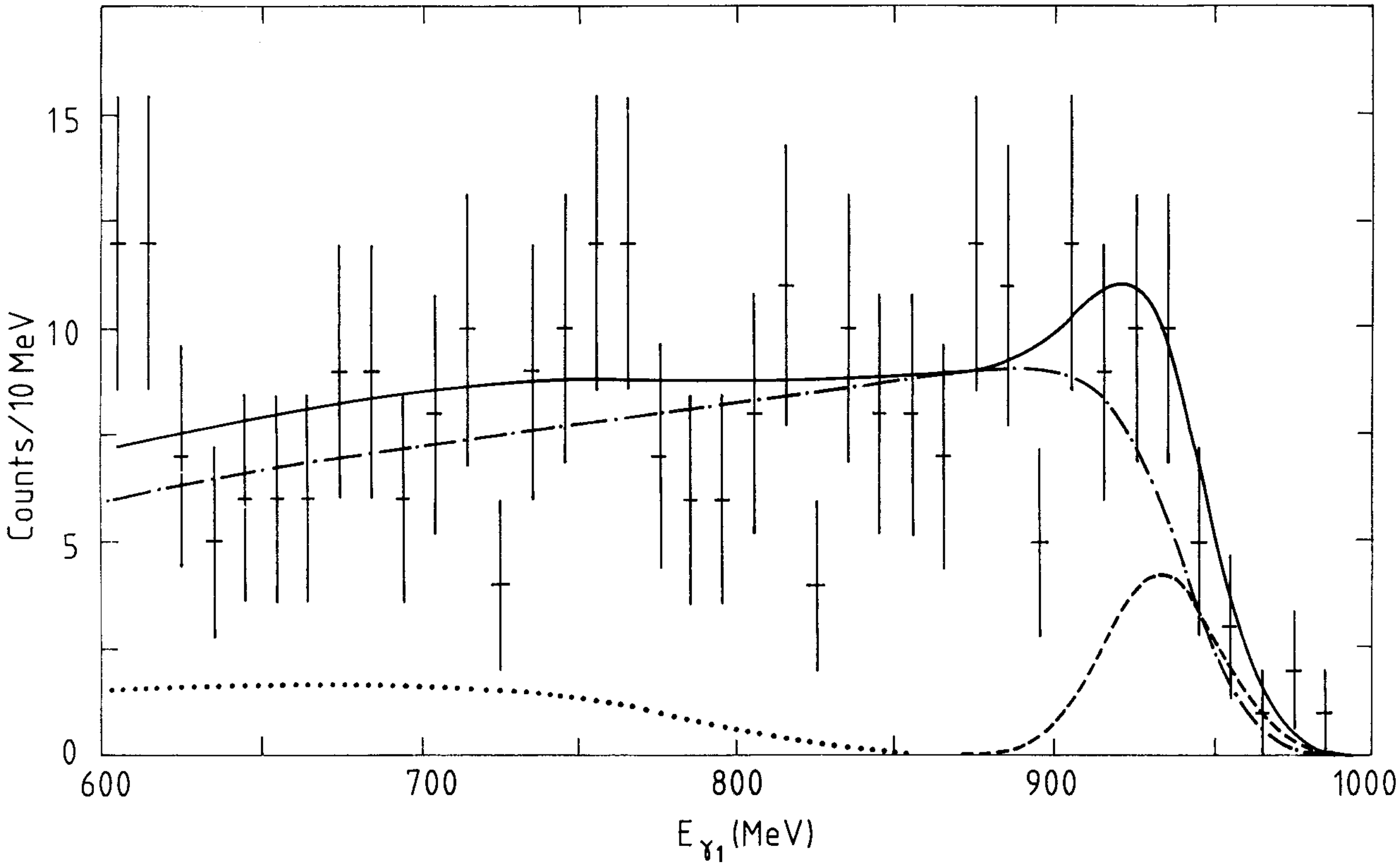

Fig. 2

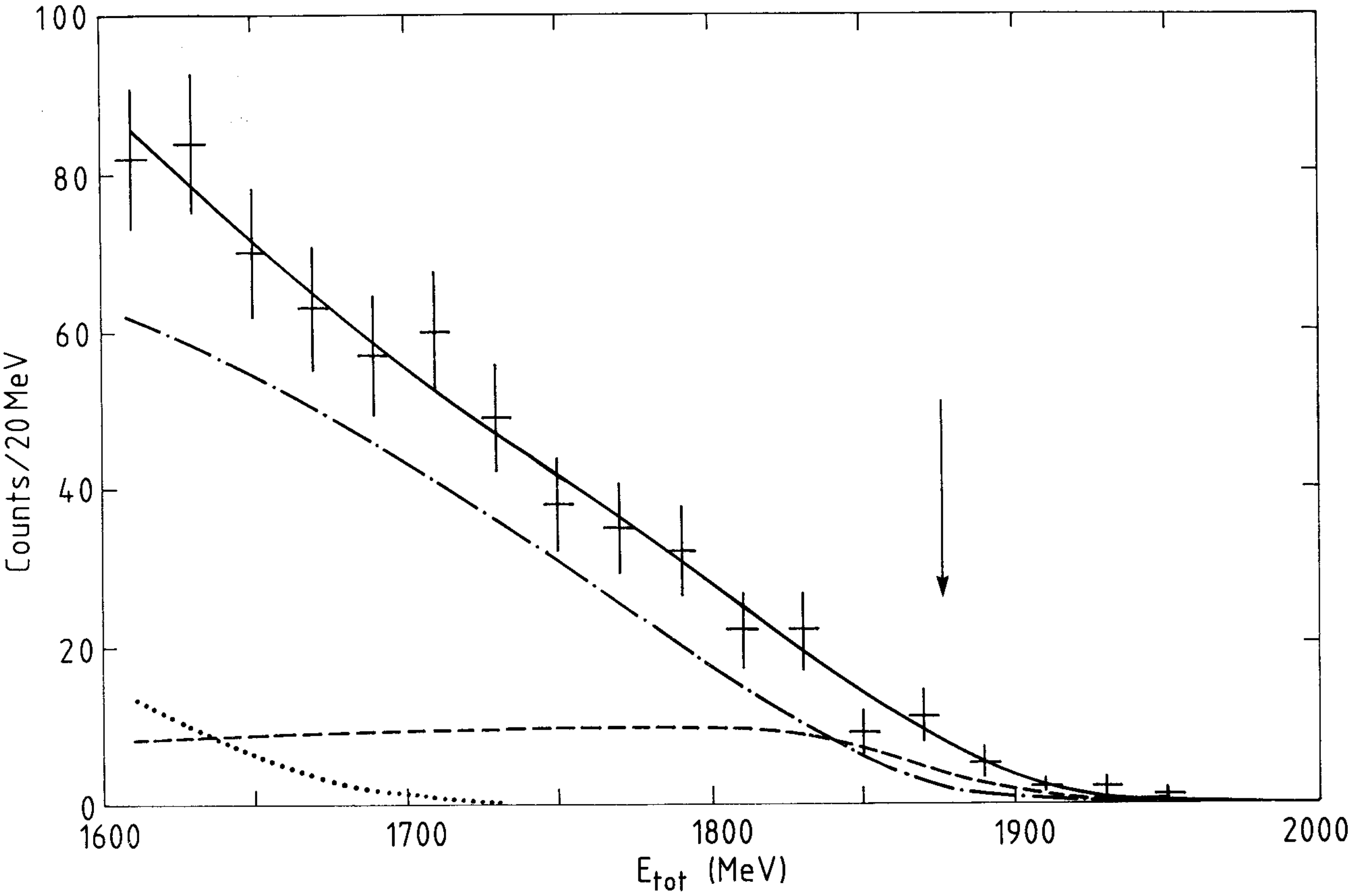

100
80
60
40
20
0
Counts/20 MeV
1600
1700
1800
1900
2000
E_tot (MeV)

Fig. 3